



Full length article



Microplastics alter soil structure and microbial community composition

Lanfang Han^{a,*}, Liying Chen^{a,1}, Yanfang Feng^b, Yakov Kuzyakov^{c,d}, Qi'ang Chen^a, Sibozhang^a, Liang Chao^a, Yanpeng Cai^a, Chuanxin Ma^a, Ke Sun^{e,*}, Matthias C. Rillig^{f,g}

^a Key Laboratory for City Cluster Environmental Safety and Green Development of the Ministry of Education, School of Ecology, Environment and Resources, Guangdong University of Technology, Guangzhou 510006, China

^b Institute of Agricultural Resources and Environment, Jiangsu Academy of Agricultural Sciences, Nanjing 210014, China

^c Department of Soil Science of Temperate Ecosystems, Department of Agricultural Soil Science, University of Göttingen, 37077 Göttingen, Germany

^d Peoples Friendship University of Russia (RUDN University), 117198 Moscow, Russia

^e State Key Laboratory of Water Simulation, School of Environment, Beijing Normal University, Beijing 100875, China

^f Freie Universität Berlin, Institute of Biology, Berlin, Germany

^g Berlin-Brandenburg Institute of Advanced Biodiversity Research (BBIB), Berlin, Germany

ARTICLE INFO

Handling Editor: Adrian Covaci

Keywords:

Microplastic contamination
Soil aggregation
Bacterial community structure
Microbial co-occurrence network
Soil health

ABSTRACT

Microplastics (MPs), including conventional hard-to-biodegrade petroleum-based and faster biodegradable plant-based ones, impact soil structure and microbiota in turn affecting the biodiversity and functions of terrestrial ecosystems. Herein, we investigated the effects of conventional and biodegradable MPs on aggregate distribution and microbial community composition in microhabitats at the aggregate scale. Two MP types (polyethylene (PE) and polylactic acid (PLA) with increasing size (50, 150, and 300 μm) were mixed with a silty loam soil (0–20 cm) at a ratio of 0.5 % (w/w) in a rice–wheat rotation system in a greenhouse under 25 °C for one year. The effects on aggregation, bacterial communities and their co-occurrence networks were investigated as a function of MP aggregate size. Conventional and biodegradable MPs generally had similar effects on soil aggregation and bacterial communities. They increased the proportion of microaggregates from 17 % to 32 %, while reducing the macroaggregates from 84 % to 68 %. The aggregate stability decreased from 1.4 mm to 1.0–1.1 mm independently of MP size due to the decline in the binding agents gluing soil particles (e.g., microbial byproducts and proteinaceous substances). MP type and amount strongly affected the bacterial community structure, accounting for 54 % of the variance. Due to less bioavailable organics, bacterial community composition within microaggregates was more sensitive to MPs addition compared to macroaggregates. Co-occurrence network analysis revealed that MPs exacerbated competition among bacteria and increased the complexity of bacterial networks. Such effects were stronger for PE than PLA MPs due to the higher persistence of PE in soils. Proteobacteria, Bacteroidetes, Chloroflexi, Actinobacteria, and Gemmatimonadetes were the keystone taxa in macroaggregates, while Actinobacteria and Chloroflexi were the keystone taxa in microaggregates. Proteobacteria, Actinobacteria, and Chloroflexi were the most sensitive bacteria to MPs addition. Overall, both conventional and biodegradable MPs reduced the portion of large and stable aggregates, altering bacterial community structures and keystone taxa, and consequently, the functions.

1. Introduction

Plastics are discarded into the environment and become fragmented into microplastics (MPs) due to natural or anthropogenic factors such as mechanical breakdown (plowing, drying/rewetting, freezing/warming, etc.) (Sipe et al., 2022), chemical oxidation and hydrolysis (He et al., 2023), and microbial/enzymatic degradation (Chen et al., 2021). As a

type of emerging contaminant that is ubiquitous in natural ecosystems, MPs have been recognized as a global change factor (Machado et al., 2018a). With the emerging evidence of the substantial accumulation of MPs in soils, e.g., up to 7 wt% (Fuller and Gautam, 2016), research attention has extended to terrestrial ecosystems (Surendran et al., 2023). MPs in soils vary in shape, size, and polymer type (e.g., polyethylene (PE), polystyrene (PS), polypropylene (PP), and polyvinyl chloride

* Corresponding authors.

E-mail addresses: hanlanfang@gdut.edu.cn (L. Han), sunke@bnu.edu.cn (K. Sun).

¹ These two authors contributed equally to this work.

(PVC)). Among these plastics, PE has been frequently detected in soils due to the use of plastic mulching in agricultural practices (Kasirajan and Ngouajio, 2012; Liu et al., 2018). In recent years, biodegradable plastics have been developed as alternatives to conventional plastics (Fan et al., 2022; Shi et al., 2022), with polylactic acid (PLA) having the highest global production capacity of plastics (31.0 %) (Bioplastics, 2023). The rapid accumulation of multiple types of MPs has a complex and profound impact on soil structures and biota. For example, it has been reported that MPs could not only act as the carriers of bacteria but also serve as carbon substrates for microbes, altering soil microbial community structure and thus affecting biogeochemical cycling (Seeley et al., 2020; Pham et al., 2021).

Aggregates, which are fundamental components of soil structure, serve as a habitat for the cycling of microbially mediated soil organic carbon (SOC) (Abiven et al., 2009; Yudina and Kuzyakov, 2023). The chemical structure, sequestration potential of SOC and soil microbial community structure depend on aggregate sizes, including macroaggregates (>0.25 mm) and microaggregates (<0.25 mm) (Six et al., 2004). For instance, *K*-selected bacteria (oligotrophs) are more likely to be found in microaggregates, whereas macroaggregates with fast turnover rates are usually inhabited by *r*-selected species (copiotrophs) (Trivedi et al., 2017; Kravchenko et al., 2021). In comparison with their macroaggregate counterparts, microaggregates have lower porosity and oxygen availability (Yudina and Kuzyakov, 2023) and are typically associated with greater amounts of physically protected and recalcitrant SOC, such as aromatics (Six et al., 2004). In addition to aggregate size distribution, aggregate stability is another frequently measured indicator, which is a widely acknowledged determinant of soil structure formation and health (Amezketta, 1999). Thus, shifts in soil aggregate size distribution and stability have profound implications for element cycling.

The size distribution and stability of soil aggregates are affected by many factors, including organic matter input, clay mineralogy, and microbial populations (Yudina and Kuzyakov, 2023). Among them, organic matter and microbial populations are two of the important factors determining aggregation by affecting microbial metabolism, leading to changes in the abundance of microbially derived metabolites (Liang et al., 2021). Microbially derived SOC can act as a binding agent that facilitates aggregate stabilization (Liang et al., 2021; Agnihotri et al., 2022). Since the main component of MPs is organic carbon, it may serve as an additional source of carbon for microbes; indeed, it has been shown from marine and soil systems that there are microbes utilizing plastic polymers (Zhang et al., 2021; Taipale et al., 2022). MPs also affect the available pore space in soil and hence the habitats of soil microbes (Machado et al., 2018a). Therefore, MPs may alter the microbial population structure, thereby affecting the formation of aggregates. To date, several studies have already explored the impacts of MPs on soil aggregation (Hou et al., 2021). For example, MP fiber incorporation decreased aggregate stability (Machado et al., 2018b). However, although MPs of varying sizes and biodegradability are present in soils, current research has predominantly concentrated on conventional MPs such as PE, PS, and PP (Liu et al., 2017; Reay et al., 2023), limiting our understanding of the effects of biodegradable MPs on aggregate formation, distribution and stability. Although the effects of conventional and biodegradable MPs on soil–plant health have been investigated (Hu et al., 2022; Song et al., 2023), little is known about their comparative effects on aggregate distribution. These knowledge gaps hinder accurate predictions of the ecological and environmental risks associated with conventional and biodegradable MPs in soils.

Therefore, we examined the effects of conventional and biodegradable MPs on soil structure (comprehensive assessment of aggregate size distribution, stability, and SOC compositions) and bacterial communities depending on aggregate size classes. We hypothesized that MPs, particularly conventional MPs, reduce the formation of large and stable aggregates by changing aggregate-associated SOC structures and/or bacterial community structure. As a common type of conventional and

biodegradable MP, PE and PLA were adopted, and the sizes of 50, 150, and 300 μm were used in the consideration of the ranges of MP size (25–5000 μm) reported in previous studies (Liu et al., 2018; Zhang et al., 2020). Specifically, we aimed to (1) evaluate the impacts of conventional and biodegradable MPs with increasing sizes on soil aggregation; (2) comprehend the compositions of bacterial communities depending on aggregate size classes under the impact of MPs; and (3) identify taxa that sensitively responded to MPs and their potential links to shifts in soil structure.

2. Materials and methods

2.1. Soil and microplastic preparation

The soils were collected from paddy fields located in Nanjing, Jiangsu Province, China. The soils were air-dried, sieved through a 2-mm sieve, and mixed thoroughly. According to the USDA-NRCS soil texture classes, the soil was a silty loam. The basic properties of the soils were as follows: pH (H_2O), 7.3; SOC, 8.8 g kg^{-1} ; cation-exchange capacity (CEC), 16.7 cmol kg^{-1} ; total nitrogen (TN), 1.0 g kg^{-1} ; available phosphorus (P), 42.3 mg kg^{-1} , and available potassium (K), 92.2 mg kg^{-1} . PE and PLA (size: 50, 150 and 300 μm) were purchased from Guangzhou Huayu Environmental Technology, Inc. (Guangzhou, China). They were abbreviated as PE50, PE150, PE300, PLA50, PLA150, and PLA300. Prior to the soil column experiments, the purchased MPs were washed three times with deionized water and freeze-dried rather than high-temperature dried to prevent structural modification. The characterizations including elemental compositions, and specific surface area of PE and PLA MPs are provided in Table S1.

2.2. Experimental design

MP effects on soil structure were investigated in the greenhouse at Jiangsu Academy of Agricultural Sciences during a one-year rice and wheat crop rotation (June 2021–May 2022), which is one of the largest agricultural production systems in many countries (Bai et al., 2016). This experiment used a soil column 30 cm in diameter and 50 cm in height (Fig. S1). The soil columns were rinsed three times with ultrapure water before use to avoid potential background contamination by MPs. There were seven treatments including a control soil with no MPs amendment and soils with MPs (PE50, PE150, PE300, PLA50, PLA150, and PLA300, respectively). For both control and MPs-amended soils, three replicates were established.

As shown in Fig. S1, MPs were mixed with topsoil (0–20 cm) (10 kg) at a ratio of 0.5 % (w/w), which is within the environmental content range (<7.0 % (w/w)) of MPs in soils (Machado et al., 2018b; Xu et al., 2020). Based on average particle size and polymer density, the number of MPs was estimated (Table S2) (Everaert et al., 2018). The estimation details are provided in the supplementary materials. On June 19, 2021, three rice plants (*Oryza sativa* L., Nangeng 46) were transplanted into each soil column along with basal fertilizer (BF). The BF consisted of 96 kg N ha^{-1} urea, 96 kg P ha^{-1} calcium superphosphate and 192 kg K ha^{-1} potassium chloride. In addition, a first supplemental fertilizer (SF1) of 96 kg N ha^{-1} and a second supplemental fertilizer (SF2) of 48 kg N ha^{-1} urea were applied on 3 July 2021 and 14 August 2021, respectively.

Water levels were maintained at 3–5 cm flooding, and a mid-season drainage was performed from 1 to 7 August 2021. Following the rice harvest on 31 August 2021, wheat (Ningmai 13) was transplanted into each column, with 30 plants per column. The wheat was harvested on May 21, 2022. As in the rice-growing season, N fertilizer was applied three times at a ratio of 3:3:4 for BF/SF1/SF2. Prior to the transplanting on December 19, 2021, BF was applied at a rate of 48 kg N ha^{-1} , 96 kg P ha^{-1} , and 192 kg K ha^{-1} . Soil moisture was maintained at 60–70 % of the water-holding capacity, following the guidelines of the International Organization for Standardization (ISO) 11274.

After the wheat harvest, soil samples were collected from the topsoil

(0–20 cm) of each column for subsequent analysis. The samples were divided into two portions: one portion was immediately stored at -20°C for soil microbial analysis, while the other portion was air-dried for the analysis of aggregate fractionation, dissolved organic carbon (DOC) characterization and SOC.

2.3. Aggregate size distribution and analysis of dissolved organic carbon

To fractionate the soil for aggregate size classes, a dry-sieving method was adopted based on the work by Schutter and Dick (2002) to allow for the determination of habitat influences on soil microorganisms. Briefly, ~ 200 g of soil was placed on nested sieves and mechanically shaken at $200\text{--}250$ oscillations min^{-1} for 2 min to divide the soil into five aggregate size classes: >2 mm (large macroaggregates), $1\text{--}2$ mm (intermediate macroaggregates), $0.25\text{--}1$ mm (small macroaggregates), $0.053\text{--}0.25$ mm (large microaggregates) and <0.053 mm (small microaggregates). Shaking for 2 min has been shown to be adequate for isolating soil aggregates without causing mechanical damage to the larger fractions (Schutter and Dick, 2002). The mean weight diameter (MWD), which acts as the indicator of structural stability of aggregates, was calculated according to the study by Zhou et al. (2020). The larger MWD indicates the higher structural stability of aggregates (Zhou et al., 2020).

DOC, which may affect aggregate formation (Chen et al., 2022), was extracted from bulk soil and aggregates with deionized water at a ratio of 1:10 (g: mL) by shaking for 48 h at 25°C . The DOC composition was assessed using three-dimensional excitation-emission matrix (3D-EEM) spectroscopy (Shimadzu RF-6000, Japan).

2.4. Soil properties, DNA extraction and MiSeq sequencing

The SOC of bulk soil was determined by oxidation using $\text{K}_2\text{Cr}_2\text{O}_7\text{--H}_2\text{SO}_4$ and titration with Fe_2SO_4 (Islam and Weil, 1998). Microbial DNA was extracted from the soils (including bulk and aggregate soils with/without the addition of PE150 and PLA150) using the E.Z.N.A.® soil DNA Kit (Omega Biotek, Norcross, GA, USA) and analyzed in triplicate. To amplify the V3-V4 hypervariable regions of the bacterial 16S rRNA gene, a thermocycler PCR system (GeneAmp 9700, ABI, USA) was utilized with primers 338F ($5'\text{-ACTCCTACGGGAGGCAGCAG-3'}$) and 806R ($5'\text{-GGACTACHVGGGTWTCTAAT-3'}$). The purified amplicons were equimolarly pooled and subjected to paired-end sequencing on an Illumina MiSeq platform (San Diego, USA). QIIME software (v 1.9.0) was used to analyze the raw data. The raw sequences of all samples were filtered, denoised, merged and nonchimeric to define amplicon sequence variants (ASVs) through the amplicon denoising algorithm (DADA2) method of the QIIME2 pipeline (<https://www.qiime2.org/>). Species classification of ASVs was based on the sklearn algorithm with reference to the Greengenes database.

2.5. Data analysis

Analysis of variance (ANOVA) was conducted using the Fisher LSD multiple comparison method, with a p value of less than 0.05 considered statistically significant. Data analysis, plotting, and correlation analysis were performed using GraphPad Prism 9.3.1 (GraphPad Software, USA) and OriginPro 2023 (Origin Lab, USA). The removecat tool in MATLAB R2021A (MathWorks Inc., USA) and the “starDom” package in R4.1.2 software were utilized to analyze the three-dimensional fluorescence data.

The individual and interactive effects of PE and PLA with aggregate size on the bacterial community composition were detected using permutational multivariate analysis of variance (PERMANOVA). To map the relative abundance of bacterial communities, TBTtools software was used (Chen et al., 2020). The structural changes of bacterial communities were evaluated using principal coordinate analysis (PCoA) based on weighted UniFrac distances. Interactions between bacterial

communities were visualized through co-occurrence networks (Spearman's $\rho > 0.8$ and $p < 0.01$). Prior to correlation analysis, microbial ASVs present in at least 75 % of the samples were screened out.

For network visualization, the R package “igraph” was employed for analysis, and Gephi software was used for plotting (Csardi and Nepusz, 2006). To quantify the degree of node connectivity, including within-module connectivity (Z_i) and among-module connectivity (P_i), the integrated network analysis pipeline (iNAP), an online analysis pipeline, was employed. The roles of network nodes were assigned based on Z_i and P_i : module hubs ($Z_i > 2.5$, $P_i < 0.625$), connectors ($Z_i < 2.5$, $P_i > 0.625$) and network hubs ($Z_i > 2.5$, $P_i > 0.625$), which are considered to play important roles in the ecosystem (Csardi and Nepusz, 2006). In addition, gene significance (GS: indicating the association of genes with environmental traits) and module membership (MM: indicating the association of genes with modules) were calculated. Keystone taxa were identified based on the following conditions: $Z_i > 2.5$ or $P_i > 0.625$; $\text{GS} > 0.6$; $\text{MM} > 0$ (Guimera and Amaral, 2005).

3. Results

3.1. Soil aggregate size distribution and stability

The SOC content with MP addition increased from 9.3 g kg^{-1} to 12.3 g kg^{-1} for PE-MPs and 11.8 g kg^{-1} for PLA-MPs ($p < 0.05$, Fig. S2). In comparison to PE150, the SOC content of PLA150 was lower by 14 % ($p < 0.05$). The control soil was mainly composed of macroaggregates, which accounted for 84 % of the soil mass. With MP addition, the portion of macroaggregates strongly decreased, and microaggregates increased (Fig. 1). With MP addition (except PLA300), the macroaggregate portion declined from 84 % to 65–71 %, while the microaggregates increased from 17 % to 29–35 % ($p < 0.05$ at sizes > 2 mm, $1\text{--}2$ mm and $0.053\text{--}0.25$ mm) (Fig. 1a and b). The MWD was also reduced from 1.4 mm to 1.0–1.1 mm due to MPs ($p < 0.05$) (Fig. 1b). The above changes triggered by MP addition were generally independent of MP type (conventional versus biodegradable) and particle size ($p > 0.05$).

3.2. DOC of aggregate size classes

PE MPs and PLA MPs decreased the DOC amounts of bulk soils from 117 mg kg^{-1} to 104 mg kg^{-1} and 97 mg kg^{-1} , respectively ($p < 0.05$ for PE300, PLA50 and PLA150) (Fig. S3). MPs had opposite impacts on the DOC contents of <0.053 mm and >2 mm aggregates. Each MP type increased the DOC contents of >2 mm aggregates ($p < 0.05$ for all PE MPs and PLA150) but lowered the DOC of <0.053 mm aggregates ($p < 0.05$ for all PE MPs, PLA150 and PLA300). In contrast, there was no significant regular pattern seen for the effects of MP particle size and type.

The DOC structure altered by MPs was evaluated by 3D-EEM analysis (Figs. 2, S4 and S5). Five regions representing tyrosine-like substances, tryptophan-like substances, fulvic substances, microbial byproducts and humic substances were obtained. All soils contained 78–86 % humic substances, 6.5–10 % microbial byproducts, 5.8–10 % fulvic substances, 0.7–1.8 % tryptophan substances, and 0.1–1.3 % tyrosine substances (Figs. 2 and S4), showing that humic substance was the primary component of DOC regardless of MP addition. With the MPs, the content of humic substances increased under each MP addition, while those of the remaining four components were reduced ($p < 0.05$ for all PE MPs and PLA50) (Figs. 2 and S4). Such change patterns were observed for bulk soils and aggregates. The EEMs in combination with PARAFAC yielded four fluorescent components (components C1, C2, C3 and C4). Among these four components, the fluorescence intensities of proteinaceous substances (C4) tended to be lower under MP addition ($p < 0.05$) (Fig. S5 and Table S3), which was consistent with the decreased abundance of tyrosine- and tryptophan-like species.

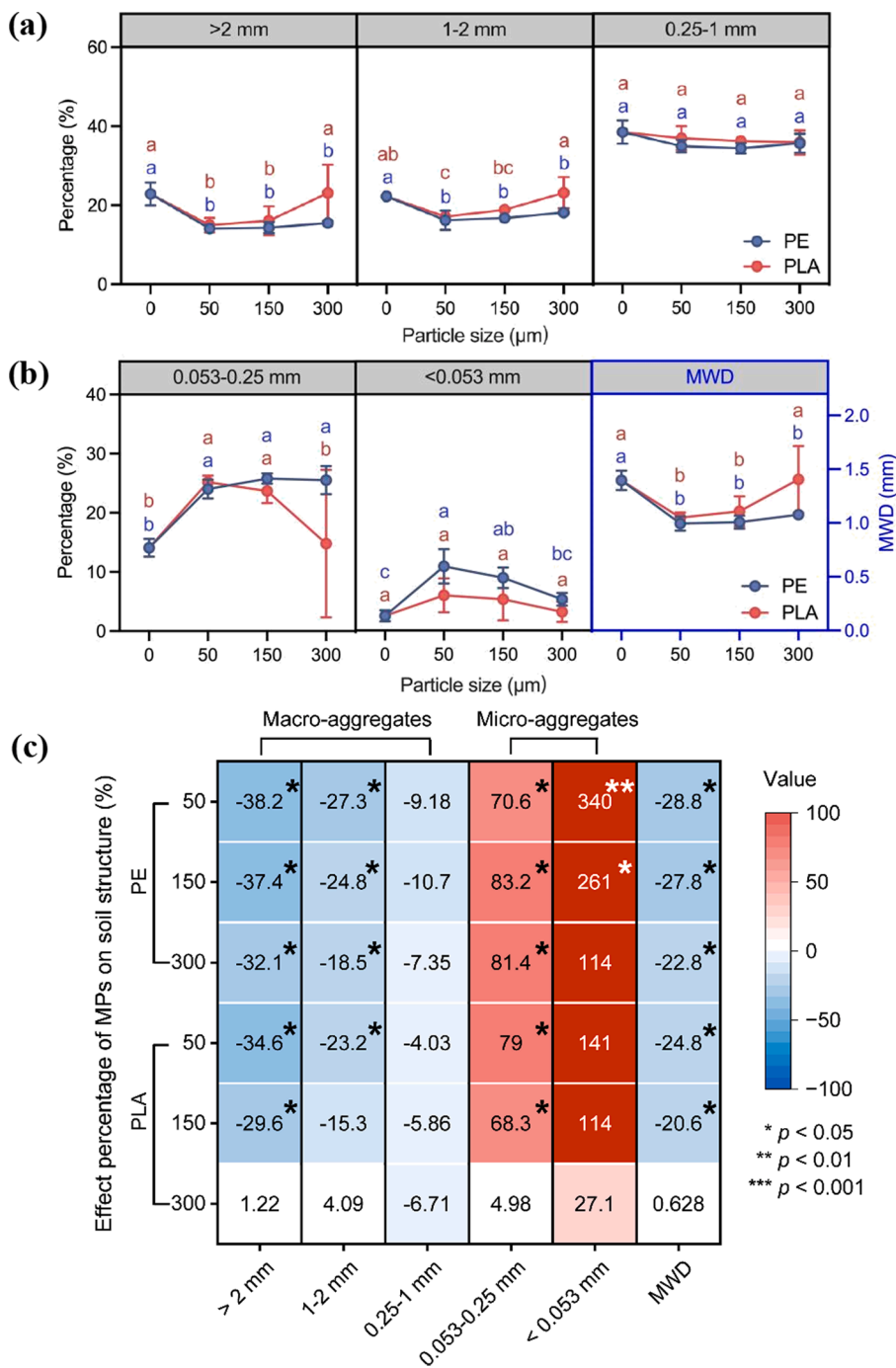


Fig. 1. Percentage of macro- (a) and micro-aggregates as well as mean weight diameter (MWD) of soil aggregates (b); the heatmap of the effects of microplastics (MPs) on aggregate size distribution and stability (c). The effect percentage for MPs is the unpaired mean differences in the percentage mass of soil aggregates between MPs and control soil. Red square and positive value represent positive effect, while blue square and negative value represent negative effect. The blue and red letters above each point indicate significant differences of PE- and PLA-added soils with control soils, respectively ($p < 0.05$). Asterisk (*) indicates a statistically significant effect (* for $p < 0.05$, ** for $p < 0.01$, *** for $p < 0.001$). Data are shown as mean \pm SD ($n = 3$). Note that PE and PLA represent the soils with polyethylene and polylactic acid MPs addition, respectively; 50, 150, 300 refer to the particle sizes of MPs. (For interpretation of the references to colour in this figure legend, the reader is referred to the web version of this article.)

3.3. Bacterial community structure across aggregate size fractions

The alpha diversity parameters, including Faith's PD, observed ASVs, and Shannon's indices, were calculated to compare the community richness and diversity in response to the addition of MPs. PE and PLA MP soils showed similar values of Faith's PD, observed ASVs, and Shannon's indices of bulk soils and aggregates ($p > 0.05$) (Fig. S6). Nonetheless, the PCoA result suggested that MP addition strongly altered bacterial

communities by forming a distinctive group different from the control soil, regardless of aggregate size (Fig. 3a), and the impact of PE MPs was similar to that of PLA MPs. The bacterial communities of micro-aggregates were distinctly separated from those of bulk soils and macroaggregates, showing that aggregate size also had a substantial influence on bacterial communities. MP addition explained approximately 54 % of the variation in the bacterial community structure ($p < 0.01$), which was much higher than that of aggregate size (14–16 %)

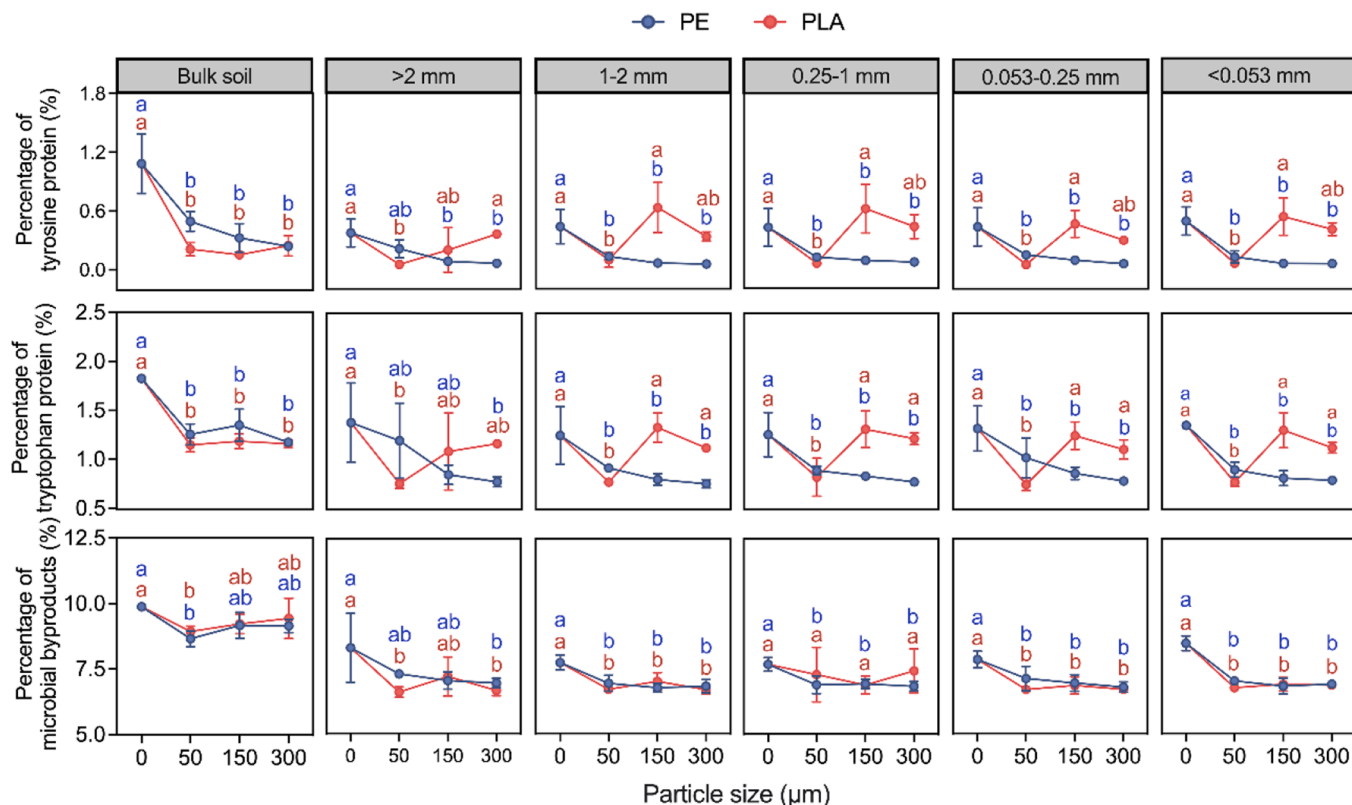


Fig. 2. Percentage of tyrosine-, tryptophan- protein and microbial byproducts in dissolved organic carbon. Data are shown as mean \pm SD ($n = 3$). The blue and red letters above each point indicate significant differences of PE- and PLA-added soils with control soils, respectively ($p < 0.05$). Note that PE and PLA represent the soils with polyethylene and polylactic acid microplastics addition, respectively. (For interpretation of the references to colour in this figure legend, the reader is referred to the web version of this article.)

(Fig. 3c).

Venn diagram analysis based on ASVs was performed to measure the overlap between the bacterial communities (Fig. S7). The number of shared ASVs was 333 for the intersection among all soils. For both bulk soil and aggregate soil of <0.053 mm and 0.25–1 mm, the unique ASV numbers all followed the order of control $>$ PLA MPs $>$ PE MPs, showing that MPs, especially PE MPs, decreased the unique ASV numbers. For the same MP addition, the macroaggregates contained more unique ASVs than the corresponding microaggregates. Fig. 3b and Table S4 depict bacterial community compositions at the phylum level with MP addition. Actinobacteriota (23–31 %), Proteobacteria (21–41 %), Acidobacteriota (7–15 %), Chloroflexi (6–12 %), Firmicutes (9–11 %), and Bacteroidota (5–7 %) were the dominant phyla in bulk soil and aggregates. The effects of MPs on bacterial composition were more obvious in < 0.053 mm aggregates, in which PE and PLA MPs consistently depleted Proteobacteria but regularly enriched Actinobacteria, Acidobacteriota, Chloroflexi, Nitrospirota, Patescibacteria, Desulfobacterota, and Cyanobacteria ($p < 0.05$) (Table S4). The bacterial community compositions were generally similar for PE and PLA MPs, with some exceptions. For instance, in the 0.25–1 mm aggregate soil, PLA MPs contained more Planctomycetota ($p < 0.05$) but fewer Nitrospirota and Firmicutes ($p < 0.05$).

3.4. Bacterial co-occurrence network across aggregate size fractions

Bacterial co-occurrence networks were constructed for bulk soil and aggregates to gain insight into the interactions among bacteria and identify the keystone species. The PE and PLA MP-amended soils formed their own distinctive bacterial networks, which differed profoundly from that of the control (Fig. S8). Multiple network topology parameters (i.e., nodes, edges, and linkage density), which represent the size and

complexity of bacterial networks, illustrated the marked difference between control and MP-amended soils. The PE and PLA MP networks incorporated 321 nodes and 700 edges and 327 nodes and 383 edges (Fig. S8 and Table 1), respectively, and were clearly higher than the network in the unamended control soil (233 nodes and 317 edges). PE MPs caused an increase in the edges and linkage density of the bacterial network by 121 % and 60 %, respectively, which were greater than those for PLA MPs (21 % and 14 %). The interactions between nodes changed with MP incorporation from mostly positive to negative, particularly for PE MPs, which induced an increase in negative links from 7 % to 45 % (Table 1).

Soil aggregate size also affected co-occurrence patterns (Fig. S9). The network pattern of the >2 mm aggregate class contained the fewest nodes and edges and the lowest linkage density of bacterial networks among all aggregate sizes (Fig. S9). There was a greater number of negatively correlated edges among bacterial communities in microaggregates (50 %) than in macroaggregates (33–35 %). Additionally, the influential (keystone) taxa under MP impact changed across aggregate classes, i.e., in macroaggregates, the keystone taxa were Proteobacteria, Bacteroidetes, Chloroflexi, Actinobacteria, and Gemmatimonadetes, while in microaggregates, the keystone taxa were Actinobacteria and Chloroflexi (Fig. 4).

3.5. Links among soil properties, aggregates, organic matter structure and bacterial community

The DOC structure was associated with aggregate size distribution and stability ($p < 0.05$) (Fig. S10). The macroaggregate (>2 mm, 1–2 mm, and 0.25–1 mm) amount and MWD increased with the content of proteinaceous substances and microbial byproduct analogs ($p < 0.05$). In contrast, the number of microaggregate (0.053–0.25 mm and $<$

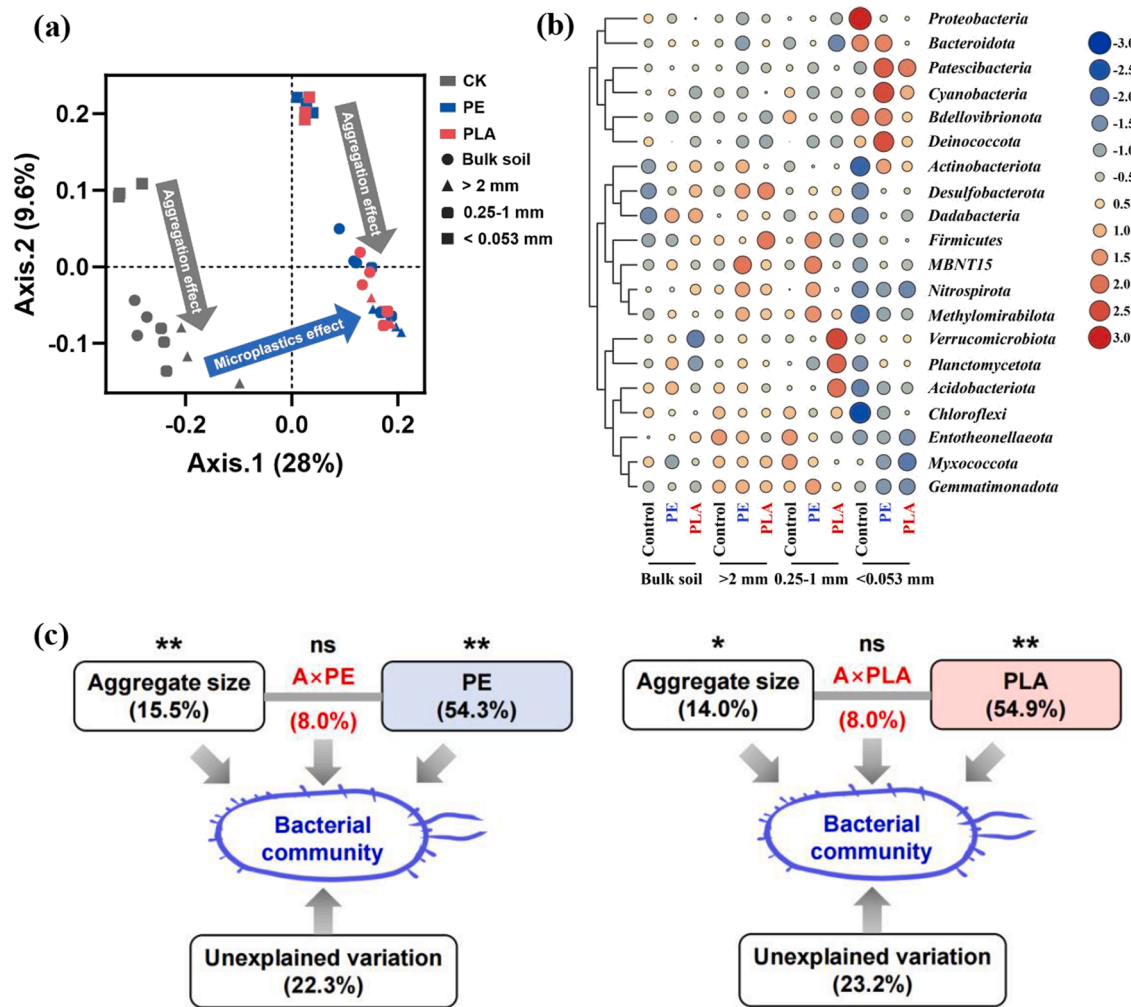


Fig. 3. Effects of microplastics (MPs) on soil bacterial community structure (a) and taxonomic structure (b) depending on aggregate size. The individual and interactive effects of soil aggregate size and PE/PLA on the bacterial community composition are tested by permutational multivariate analysis of variance (PERMANOVA) in permutations (c). The relative abundance of bacterial communities is normalized. Note that PE and PLA represent the soils with 150 μm of polyethylene and polylactic acid MPs addition, respectively. * $p < 0.05$; ** $p < 0.01$; *** $p < 0.001$; ns, no significant difference.

Table 1
Topological properties of co-occurring bacterial networks.

	Bacterial community				Samples		
	Soil aggregate sizes						
Network metric	Bulk soil	>2 mm	0.25–1 mm	<0.053 mm	Control	PE	PLA
Total nodes	340	309	383	351	233	321	327
Total links	643	467	697	675	317	700	383
Positive links	71.2 %	64.7 %	67.4 %	50.1 %	92.7 %	55.1 %	62.1 %
Negative links	28.8 %	35.3 %	32.6 %	49.9 %	7.3 %	44.9 %	37.9 %
Linkage density	1.89	1.51	1.82	1.92	1.36	2.18	1.17
Average degree	3.78	3.02	3.64	3.85	2.72	4.36	2.34
Average clustering coefficient	0.27	0.18	0.24	0.19	0.26	0.20	0.13
Average path distance	5.28	6.19	6.24	5.78	3.87	4.71	8.69
Graph density/ 10^2	1.12	0.98	0.95	1.10	1.17	1.36	0.72
Number of modules	44	51	52	46	48	53	65
Modularity	0.74	0.71	0.73	0.69	0.78	0.57	0.81

Note that control group represents the soil with no microplastics (MPs) addition; PE and PLA represent the soils with 150 μm of polyethylene and polylactic acid MPs addition, respectively.

0.053 mm) was inversely related to the abundance of proteinaceous substances, microbial byproduct analogs, and fulvic acid ($p < 0.01$), but positively correlated with the content of humic acid ($p < 0.01$). Additionally, these structures had strong links with the abundance of several keystone taxa (e.g., ASV24 (Actinobacteria), ASV305 (Proteobacteria))

of bulk soils and aggregates ($p < 0.05$) (Fig. S11). Specifically, abundance of ASV24 (Actinobacteria) in bulk soils decreased as the increase of proteinaceous substances, microbial byproduct analogs, and fulvic acid content ($p < 0.01$). ASV218 (Chloroflexi) and ASV305 (Proteobacteria) in >2 mm aggregates as well as ASV145 (Gemmatimonadetes),

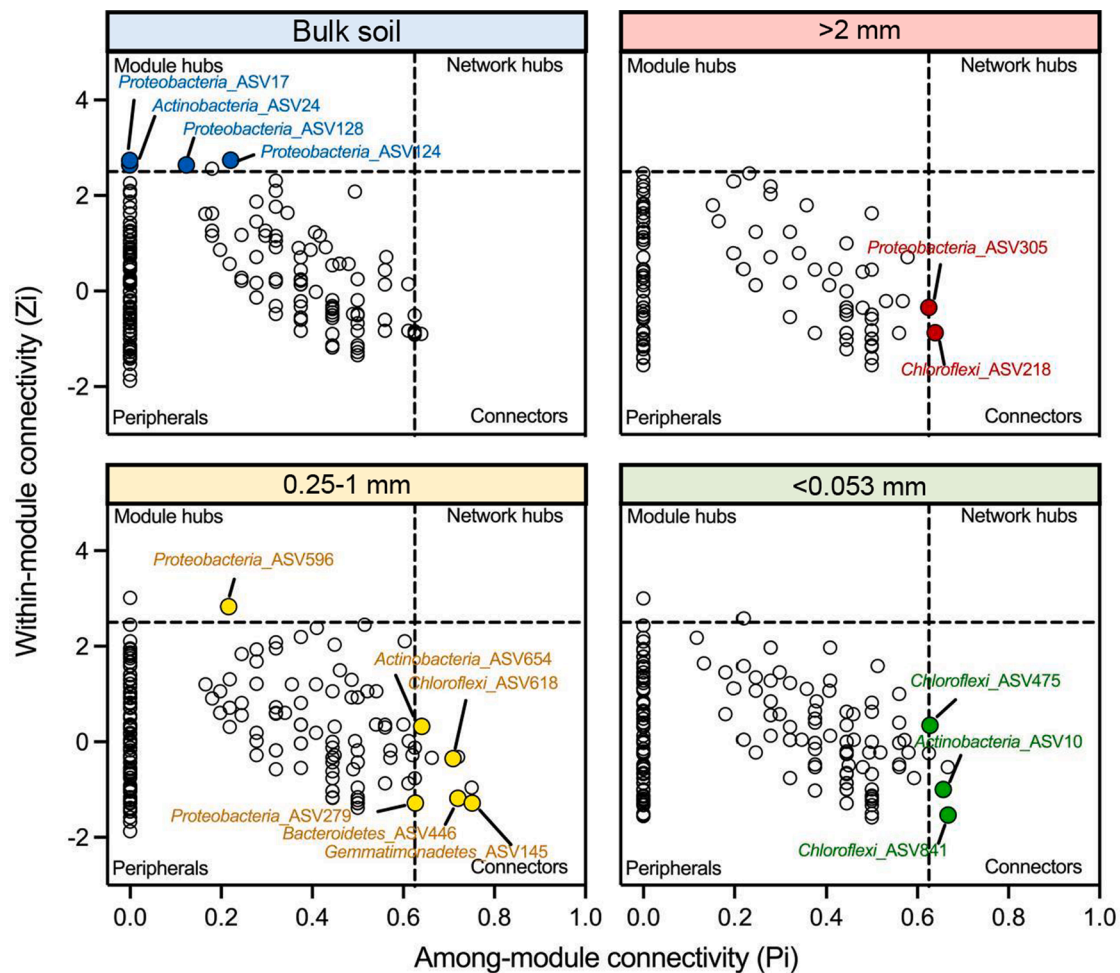


Fig. 4. Distribution of keystone taxa (colored nodes) indicated by two topological parameters namely within-module connectivity (Z_i) and among-module connectivity (P_i) of bacterial networks. The threshold values of Z_i and P_i for categorizing species are 2.5 and 0.625, respectively. $Z_i > 2.5$ and $P_i < 0.625$: module hubs; $Z_i > 2.5$ and $P_i > 0.625$: network hubs; $Z_i < 2.5$ and $P_i > 0.625$: connectors; $Z_i < 2.5$ and $P_i < 0.625$: peripherals. The nodes, which are in the regions of module hubs, network hubs or connectors, and also follow the conditions of gene significance > 0.6 (GS: gene-environmental trait association) as well as module membership > 0 (MM: gene-module association) were colored and labelled with the corresponding phylum and ASV ID.

ASV446 (Bacteroidetes), ASV618 (Chloroflexi), and ASV654 (Actinobacteria) in 0.25–1 mm aggregates were negatively correlated with the content of microbial byproduct analogs ($p < 0.01$). In terms of < 0.053 mm aggregates, ASV10 (Actinobacteria), ASV475 (Chloroflexi), and ASV841 (Chloroflexi) were inversely related to the amount of microbial byproduct analogs ($p < 0.001$).

4. Discussion

4.1. Conventional and degradable MPs altered aggregate size distribution and the DOC structure

MPs increased the SOC content, but this increase by PLA (1.6–3.1 g kg^{-1}) and PE (2.8–3.3 g kg^{-1}) MPs did not correspond to the added MP-C amounts (PLA: 2.0 g C kg^{-1} ; PE: 4.25 g C kg^{-1}). Typically, the average SOC content in PLA300 soil was slightly higher than that of PE300, although PE had almost twice the carbon content (85 %) compared to PLA (40 %). This suggests that other processes, such as altered bacterial community structure (discussed below), might contribute to the shifts in SOC in MP-added soils by mediating carbon cycling processes (Lin et al., 2019). Conventional and degradable MPs increased the microaggregate proportion and reduced the macroaggregate amount, regardless of MP type (conventional versus biodegradable) and particle size (Fig. 1). This is partly explained by the fact that the sizes of most MPs were in the

microaggregate range (< 0.25 mm). However, this cannot fully account for the phenomenon since MPs with a size of 300 μm (macroaggregates) also reduced the macroaggregate fraction. Zhang and Liu (2018) reported that MPs mainly accumulated in microaggregates rather than macroaggregates. According to the soil aggregation model (Six et al., 2004), MP-enriched microaggregates could not be incorporated well into macroaggregates (> 0.25 mm). This is because MPs, particularly PE, do not carry surface charges that are essential for the physicochemical bonding (e.g., hydrogen bonds, electrostatic attraction, ligand exchange, and van der Waals forces) of mineral components and microbially derived extracellular polysaccharides (Wei et al., 2012). The inclusion of MPs in aggregates could result in fracture points, weakening or breaking of the bonds that bind solids together (Garland et al., 2023). Thus, many of the weakly bound aggregates (i.e., macroaggregates) eventually disintegrate, reducing overall stability, as evidenced by the decrease in MWD.

Both the SOC content and the DOC structure of bulk soil and aggregates were affected, with a reduction in the DOC content in the presence of MPs (Ma et al., 2023). This decrease was likely due to the adsorption of DOC to MP particles through mechanisms including partitioning and surface adsorption by hydrophobic interactions and van der Waals forces (Chen et al., 2018; Chen et al., 2023). MPs increased the DOC amount in aggregates larger than 2 mm but lowered the DOC of < 0.053 mm aggregates. As mentioned above, MPs tended to accumulate

in microaggregates, adsorbing DOC.

For bulk soils and aggregates, two MPs increased the levels of humic substances while reducing the microbially produced byproducts and proteinaceous species. Microbial byproducts and proteinaceous species can facilitate aggregate stabilization by acting as gluing agents (Six et al., 2004). In particular, proteinaceous substances contribute more to aggregate stability than bulk soil organic matter (Agnihotri et al., 2022). Strong and positive links between macroaggregate or structural stability and microbial byproducts or the proteinaceous fraction were noted (Fig. S10). Consequently, the decrease in microbially produced byproducts and proteinaceous compounds reduced the macroaggregate portion and structural stability.

4.2. Conventional and degradable MPs altered bacterial communities across the aggregate size classes

Aggregate size classes have specific compositions of bacterial communities (Figs. 4 and S9) due to the heterogeneity of physicochemical properties. Macroaggregates typically contain more labile substrates, e. g., particulate organic matter, while microaggregates have a higher recalcitrant SOC content (Shi et al., 2023). Additionally, MP addition had an apparently stronger influence on regulating the bacterial community structure, and moreover, the effects induced by PE and PLA MPs were similar (Fig. 3). These results underlined the central effects of conventional and biodegradable MPs on soil bacterial communities. As overviewed by Zhang et al. (2021), MPs entering soils cause a range of physical, chemical, and biological reactions that in turn impact soil properties (e.g., soil pH) and further microbial habitats. Correspondingly, the incorporation of MPs had strong effects on bacterial communities. MPs strongly influenced the bacterial compositions in all aggregate size classes, and those in <0.053 mm aggregates were more strongly influenced, suggesting that soil bacteria in the microaggregates were more sensitive to the MPs. This was likely because microaggregates contained less bioavailable organics (Shi et al., 2023), and the bacteria thus more sensitively responded to the input of exogenous organic matter.

Proteobacteria, Bacteroidetes, Chloroflexi, Actinobacteria, and Gemmatimonadetes were identified as the keystone taxa in macroaggregates, and Actinobacteria and Chloroflexi were the keystone taxa in microaggregates. These identified keystone taxa affected the DOC compositions of bulk and aggregate soils based on their strong relationships (Fig. S11). Most keystone taxa were strongly related to microbial byproduct analogs and proteinaceous species, which serve as gluing agents that facilitate aggregate stabilization (Liang et al., 2021; Agnihotri et al., 2022). Therefore, the changes in the abundance of keystone taxa under MPs indirectly affected soil aggregate stability. Among the identified keystone taxa, there was an obvious increase in the abundance of Actinobacteria in bulk soils and aggregates as well as Chloroflexi in microaggregates with MP addition, while Proteobacteria were clearly decreased (Table S4). In contrast, the abundances of Gemmatimonadetes and Bacteroidetes remained stable in the presence of both types of MPs. Consequently, Proteobacteria, Actinobacteria, and Chloroflexi were the bacterial taxa most sensitive to MP addition, and the decrease in Proteobacteria with MP addition may be attributed to its preference as an *r*-strategist in soils with higher C availability (Eilers et al., 2010). In MP soils, SOC with high C availability would be “diluted” by MPs due to their recalcitrance (Hou et al., 2021; Xiao et al., 2022). This also partly explained the increase in Actinobacteria and Chloroflexi in MP soils, considering that they are *K*-strategists that would compete well in soils with low C availability (Fierer et al., 2007). Actinobacteria and Chloroflexi were associated with low-quality resources, especially Actinobacteria, which have a fungi-like filamentous growth form and are adapted to decompose recalcitrant SOC similar to the added MPs (Fierer et al., 2007).

4.3. Conventional and degradable MPs altered bacterial co-occurrence patterns

Microbial co-occurrence patterns are very useful tools to evaluate the potential interactions between microbes and reveal the niche structure in the soil (Banerjee et al., 2018). The network topological patterns differed between the control and MP soils (Fig. S8) and macro- versus microaggregates (Fig. S9). As suggested by the positive and negative links, the interactions between nodes changed to be more negative with MP addition, and the extent of the change was comparatively stronger for PE MPs than PLA MPs (Table 1). Compared with macroaggregates, microaggregates had more negative interactions. This suggested that bacterial competition was enhanced in microaggregates and soils with MP incorporation. A decrease in labile SOC can exacerbate competition among microbes (Lin et al., 2019). As a typical structurally recalcitrant organic C, MP addition can “physically dilute” the content of labile SOC, thereby exacerbating bacterial competition. Consistent with the more refractory characteristic of PE MPs than PLA MPs, a stronger competition was found in PE MPs. Besides, as shown in Table S1, PLA MPs showed much larger specific surface area than PE MPs, and thus had a developed pore structure. The pores in PLA MPs, along with their degradability, could provide more favorable conditions for the growth of soil bacteria (Jiménez-Arroyo et al., 2023; Lu et al., 2023), thereby partly alleviating their competition relative to PE MPs. In terms of the effects of aggregate sizes, microaggregates offer more intense protection for SOC from being utilized by microbes (Han et al., 2016) and therefore display stronger competition between bacteria than inside macroaggregates.

Soil microbial network complexity has important implications for microbiome stability and ecosystem multifunctionality (Qiu et al., 2021). The addition of MPs increased bacterial network complexity, which is in line with previous reports that the complexity of microbial communities is often greater on MPs than on substrata, such as leaves, wood, and surrounding soils (Wu et al., 2019; Zhang et al., 2019). Nonetheless, comparisons of the network complexity among MP types are limited. Zhang et al. (2019) reported that the complexity of interactions between microbial groups on MPs was related to the persistence of MPs in soils. They highlighted that the longer persistence of MPs in soils was responsible for the more complex interactions between microbial groups on MPs, as a more complicated core microbiome capable of metabolizing their own substrate might be formed (Arias-Andres et al., 2018). Unlike PLA, PE MPs would not significantly hydrolyze and fragment in soils on the timescale of one year and thus showed higher persistence (Yuan et al., 2020). Consistently, this study found that the complexity of bacterial networks on PE MPs was greater than that on PLA MPs.

5. Conclusions

Conventional and biodegradable MPs influence aggregate structure and bacterial communities with consequences for functional changes in soils. A one-year incubation of conventional and biodegradable MPs with diverse particle sizes reduced aggregate size and stability from 1.4 mm to 1.0–1.1 mm, and the macroaggregate portion from 84 % to 65–71 %, partly due to the decline of microbial byproducts and proteinaceous substances that served as binding agents for soil particles. This was independent of the particle sizes of MPs. MPs induced strong effects (~54 % of the variance explained) on the bacterial community structure, suggesting central consequences for soil functions. In comparison to soil with polylactic acid (37.9 %), the soil with polyethylene (44.9 %) had more negative relationships between bacteria, indicating greater competition and less favorable habitat conditions. The keystone taxa under MP influence were dependent on the aggregate size classes. In macroaggregates, the keystone taxa were Proteobacteria, Bacteroidetes, Chloroflexi, Actinobacteria, and Gemmatimonadetes; in microaggregates, however, the keystone taxa were Actinobacteria and

Chloroflexi. These keystone taxa well explained the abundance of microbially produced organic matter in soils, in turn affecting aggregate stability. In addition, among these keystone taxa, Proteobacteria, Actinobacteria, and Chloroflexi were sensitive to MP addition.

Overall, MPs prevented the formation of large and stable aggregates through two mechanisms: 1) MPs did not carry surface charges and would create fracture points among soil solids, weakening or breaking the bonds that bind solids together; 2) through modifying the soil bacterial community, MPs decreased the abundance of microbially derived metabolites, which served as adhesive agents of soil aggregation. The effects of biodegradable MPs were similar to those of conventional MPs, suggesting that the usage of biodegradable plastics as substitutes would not efficiently lessen the risks of MPs. However, it should be noted that since the MPs were not isolated from the soils at the end of the experiment, we have not elucidated the aging and biodegradation of conventional and biodegradable MPs in soils. This prevents us from knowing which components (MP itself or the moieties released during aging) mainly contributed to the changes in soil aggregation and bacterial community structure. We thus call for future research on the degradation of MPs (especially biodegradable ones) when a long-term experiment will be conducted.

CRedit authorship contribution statement

Lanfeng Han: Writing – original draft, Validation, Resources, Project administration, Methodology, Investigation, Funding acquisition, Conceptualization. **Liying Chen:** Writing – review & editing, Visualization, Methodology, Investigation, Formal analysis, Data curation. **Yanfeng Feng:** Writing – review & editing, Supervision. **Yakov Kuzyakov:** Writing – review & editing. **Qi'ang Chen:** Writing – review & editing, Data curation. **Sibo Zhang:** Writing – review & editing, Investigation. **Liang Chao:** Writing – review & editing. **Yanpeng Cai:** Writing – review & editing, Supervision. **Chuanxin Ma:** Writing – review & editing, Investigation. **Ke Sun:** Writing – review & editing, Supervision, Project administration, Methodology, Formal analysis. **Matthias C. Rillig:** Writing – review & editing.

Declaration of competing interest

The authors declare that they have no known competing financial interests or personal relationships that could have appeared to influence the work reported in this paper.

Data availability

Data will be made available on request.

Acknowledgements

This research was supported by the National Key Research and Development Program of China (2021YFF0502803), the Key-Area Research and Development Program of Guangdong Province (2020B1111380003), National Natural Science Foundation of China (42125703, 42277203), Young Elite Scientists Sponsorship Program by CAST (2021QNR0001), and the RUDN University Strategic Academic Leadership Program.

Appendix A. Supplementary material

Supplementary data to this article can be found online at <https://doi.org/10.1016/j.envint.2024.108508>.

References

Abiven, S., Menasseri, S., Chenu, C., 2009. The effects of organic inputs over time on soil aggregate stability - a literature analysis. *Soil Biol. Biochem.* 41, 1–12.

- Agnihotri, R., Sharma, M.P., Prakash, A., Ramesh, A., Bhattacharjya, S., Patra, A.K., Manna, M.C., Kurganova, I., Kuzyakov, Y., 2022. Glycoproteins of arbuscular mycorrhiza for soil carbon sequestration: review of mechanisms and controls. *Sci. Total Environ.* 806, 150571.
- Amezketta, E., 1999. Soil aggregate stability: a review. *J. Sustain. Agric.* 14, 83–151.
- Arias-Andres, M., Kettner, M.T., Miki, T., Grossart, H.-P., 2018. Microplastics: new substrates for heterotrophic activity contribute to altering organic matter cycles in aquatic ecosystems. *Sci. Total Environ.* 635, 1152–1159.
- Bai, H., Tao, F., Xiao, D., Liu, F., Zhang, H., 2016. Attribution of yield change for rice-wheat rotation system in China to climate change, cultivars and agronomic management in the past three decades. *Clim. Change* 135, 539–553.
- Banerjee, S., Schläppli, K., van der Heijden, M.G.A., 2018. Keystone taxa as drivers of microbiome structure and functioning. *Nat. Rev. Microbiol.* 16, 567–576.
- European Bioplastics, 2023. Bioplastics market development update 2023. <https://www.european-bioplastics.org/market/>.
- Chen, C., Chen, H., Zhang, Y., Thomas, H.R., Frank, M.H., He, Y., Xia, R., 2020. TBtools: an integrative toolkit developed for interactive analyses of big biological data. *Mol. Plant* 13, 1194–1202.
- Chen, L., Han, L., Feng, Y., He, J., Xing, B., 2022. Soil structures and immobilization of typical contaminants in soils in response to diverse microplastics. *J. Hazard. Mater.* 438, 129555.
- Chen, W., Ouyang, Z., Qian, C., Yu, H., 2018. Induced structural changes of humic acid by exposure of polystyrene microplastics: a spectroscopic insight. *Environ. Pollut.* 233, 1–7.
- Chen, Q., Wang, Q., Zhang, C., Zhang, J., Dong, Z., Xu, Q., 2021. Aging simulation of thin-film plastics in different environments to examine the formation of microplastic. *Water Res.* 202, 117462.
- Chen, T., Wen, X., Li, X., He, J., Yan, B., Fang, Z., Zhao, L., Liu, Z., Han, L., 2023. Single/co-adsorption and mechanism of methylene blue and lead by beta-cyclodextrin modified magnetic alginate/biochar. *Bioresour. Technol.* 381, 129130.
- Csardi, G., Nepusz, T., 2006. The igraph software package for complex network research. *Interjournal Complex Syst.* 1695, 1–9.
- Eilers, K.G., Lauber, C.L., Knight, R., Fierer, N., 2010. Shifts in bacterial community structure associated with inputs of low molecular weight carbon compounds to soil. *Soil Biol. Biochem.* 42, 896–903.
- Everaert, G., Van Cauwenberghe, L., De Rijcke, M., Koelmans, A.A., Mees, J., Vandegehuchte, M., Janssen, C.R., 2018. Risk assessment of microplastics in the ocean: modelling approach and first conclusions. *Environ. Pollut.* 242, 1930–1938.
- Fan, P., Yu, H., Xi, B., Tan, W., 2022. A review on the occurrence and influence of biodegradable microplastics in soil ecosystems: are biodegradable plastics substitute or threat? *Environ. Int.* 163, 107244.
- Fierer, N., Bradford, M.A., Jackson, R.B., 2007. Toward an ecological classification of soil bacteria. *Ecology* 88, 1354–1364.
- Fuller, S., Gautam, A., 2016. A procedure for measuring microplastics using pressurized fluid extraction. *Environ. Sci. Technol.* 50, 5774–5780.
- Garland, G., Koestel, J., Johannes, A., Heller, O., Doetterl, S., Or, D., Keller, T., 2023. Perspectives on the misconception of levitating soil aggregates. *Egosphere* 2023, 1–15.
- Guimera, R., Amaral, L.A.N., 2005. Functional cartography of complex metabolic networks. *Nature* 433, 895–900.
- Han, L., Sun, K., Jin, J., Xing, B., 2016. Some concepts of soil organic carbon characteristics and mineral interaction from a review of literature. *Soil Biol. Biochem.* 94, 107–121.
- He, J., Han, L., Ma, W., Xu, C., Xu, E.G., Ma, C., Xing, B., Yang, Z., 2023. Mechanism insight into the facet-dependent photoaging of polystyrene microplastics on hematite in freshwater. *Water Res.* X 19, 100185.
- Hou, J., Xu, X., Yu, H., Xi, B., Tan, W., 2021. Comparing the long-term responses of soil microbial structures and diversities to polyethylene microplastics in different aggregate fractions. *Environ. Int.* 149, 106398.
- Hu, X., Gu, H., Wang, Y., Liu, J., Yu, Z., Li, Y., Jin, J., Liu, X., Dai, Q., Wang, G., 2022. Succession of soil bacterial communities and network patterns in response to conventional and biodegradable microplastics: a microcosmic study in Mollisol. *J. Hazard. Mater.* 436, 129218.
- Islam, K.R., Weil, R.R., 1998. A rapid microwave digestion method for colorimetric measurement of soil organic carbon. *Commun. Soil Sci. Plant Anal.* 29, 2269–2284.
- Jiménez-Arroyo, C., Tamargo, A., Molinero, N., Reinoso, J.J., Alcolea-Rodríguez, V., Portela, R., Bañares, M.A., Fernández, J.F., Moreno-Arribas, M.V., 2023. Simulated gastrointestinal digestion of polylactic acid (PLA) biodegradable microplastics and their interaction with the gut microbiota. *Sci. Total Environ.* 902, 166003.
- Kasirajan, S., Ngouajio, M., 2012. Polyethylene and biodegradable mulches for agricultural applications: a review. *Agron. Sustain. Dev.* 32, 501–529.
- Kravchenko, A.N., Guber, A.K., Gunina, A., Dippold, M.A., Kuzyakov, Y., 2021. Pore-scale view of microbial turnover: combining ¹⁴C imaging, μ CT and zymography after adding soluble carbon to soil pores of specific sizes. *Eur. J. Soil Sci.* 72, 593–607.
- Liang, Y., Lehmann, A., Yang, G., Leifheit, E.F., Rillig, M.C., 2021. Effects of microplastic fibers on soil aggregation and enzyme activities are organic matter dependent. *Front. Environ. Sci.* 9, 650155.
- Lin, Y., Ye, G., Kuzyakov, Y., Liu, D., Fan, J., Ding, W., 2019. Long-term manure application increases soil organic matter and aggregation, and alters microbial community structure and keystone taxa. *Soil Biol. Biochem.* 134, 187–196.
- Liu, M., Lu, S., Song, Y., Lei, L., Hu, J., Lv, W., Zhou, W., Cao, C., Shi, H., Yang, X., 2018. Microplastic and mesoplastic pollution in farmland soils in suburbs of Shanghai, China. *Environ. Pollut.* 242, 855–862.
- Liu, H., Yang, X., Liu, G., Liang, C., Xue, S., Chen, H., Ritsema, C.J., Geissen, V., 2017. Response of soil dissolved organic matter to microplastic addition in Chinese loess soil. *Chemosphere* 185, 907–917.

- Lu, S., Hao, J., Yang, H., Chen, M., Lian, J., Chen, Y., Brown, R.W., Jones, D.L., Wan, Z., Wang, W., 2023. Earthworms mediate the influence of polyethylene (PE) and polylactic acid (PLA) microplastics on soil bacterial communities. *Sci. Total Environ.* 905, 166959.
- Ma, J., Xu, M., Wu, J., Yang, G., Zhang, X., Song, C., Long, L., Chen, C., Xu, C., Wang, Y., 2023. Effects of variable-sized polyethylene microplastics on soil chemical properties and functions and microbial communities in purple soil. *Sci. Total Environ.* 868, 161642.
- Machado, A.A.S., Kloas, W., Zarfl, C., Hempel, S., Rillig, M.C., 2018a. Microplastics as an emerging threat to terrestrial ecosystems. *Glob. Chang. Biol.* 24, 1405–1416.
- Machado, A.A.S., Lau, C.W., Till, J., Kloas, W., Lehmann, A., Becker, R., Rillig, M.C., 2018b. Impacts of microplastics on the soil biophysical environment. *Environ. Sci. Technol.* 52, 9656–9665.
- Pham, D.N., Clark, L., Li, M., 2021. Microplastics as hubs enriching antibiotic-resistant bacteria and pathogens in municipal activated sludge. *J. Hazard. Mater. Lett.* 2, 100014.
- Qiu, L., Zhang, Q., Zhu, H., Reich, P.B., Banerjee, S., van der Heijden, M.G., Sadowsky, M.J., Ishii, S., Jia, X., Shao, M.J.T.I., 2021. Erosion reduces soil microbial diversity, network complexity and multifunctionality. *ISME J.* 15, 2474–2489.
- Reay, M.K., Greenfield, L.M., Graf, M., Lloyd, G.E.M., Evershed, R.P., Chadwick, D.R., Jones, D.L., 2023. LDPE and biodegradable PLA-PBAT plastics differentially affect plant-soil nitrogen partitioning and dynamics in a *Hordeum vulgare* mesocosm. *J. Hazard. Mater.* 447, 130825.
- Schutter, M.E., Dick, R.P., 2002. Microbial community profiles and activities among aggregates of winter fallow and cover-cropped soil. *Soil Sci. Soc. Am. J.* 66, 142–153.
- Seeley, M.E., Song, B., Passie, R., Hale, R.C., 2020. Microplastics affect sedimentary microbial communities and nitrogen cycling. *Nat. Commun.* 11, 2372.
- Shi, J., Sun, Y., Wang, X., Wang, J., 2022. Microplastics reduce soil microbial network complexity and ecological deterministic selection. *Environ. Microbiol.* 24, 2157–2169.
- Shi, J., Deng, L., Gunina, A., Alharbi, S., Wang, K., Li, J., Liu, Y., Shangguan, Z., Kuzyakov, Y., 2023. Carbon stabilization pathways in soil aggregates during long-term forest succession: implications from $\delta^{13}\text{C}$ signatures. *Soil Biol. Biochem.* 180, 108988.
- Sipe, J.M., Bossa, N., Berger, W., von Windheim, N., Gall, K., Wiesner, M.R., 2022. From bottle to microplastics: can we estimate how our plastic products are breaking down? *Sci. Total Environ.* 814, 152460.
- Six, J., Bossuyt, H., Degryze, S., Denef, K., 2004. A history of research on the link between (micro)aggregates, soil biota, and soil organic matter dynamics. *Soil Tillage Res.* 79, 7–31.
- Song, B., Shang, S., Cai, F.M., Liu, Z., Fang, J., Li, N., Adams, J.M., Razavi, B.S., 2023. Microbial resistance in rhizosphere hotspots under biodegradable and conventional microplastic amendment: community and functional sensitivity. *Soil Biol. Biochem.* 180, 108989.
- Surendran, U., Jayakumar, M., Raja, P., Gopinath, G., Chellam, P.V., 2023. Microplastics in terrestrial ecosystem: sources and migration in soil environment. *Chemosphere* 318, 137946.
- Taipale, S.J., Vesamaki, J., Kautonen, P., Kukkonen, J.V.K., Biasi, C., Nissinen, R., Tirola, M., 2022. Biodegradation of microplastic in freshwaters: a long-lasting process affected by the lake microbiome. *Environ. Microbiol.* 1–12.
- Trivedi, P., Delgado-Baquerizo, M., Jeffries, T.C., Trivedi, C., Anderson, I.C., Lai, K., McNee, M., Flower, K., Singh, B.P., Minkey, D., Singh, B.K., 2017. Soil aggregation and associated microbial communities modify the impact of agricultural management on carbon content. *Environ. Microbiol.* 19, 3070–3086.
- Wei, S., Tan, W., Zhao, W., Yu, Y., Liu, F., Koopal, L.K., 2012. Microstructure, interaction mechanisms, and stability of binary systems containing goethite and kaolinite. *Soil Sci. Soc. Am. J.* 76, 389–398.
- Wu, X., Pan, J., Li, M., Li, Y., Bartlam, M., Wang, Y., 2019. Selective enrichment of bacterial pathogens by microplastic biofilm. *Water Res.* 165, 114979.
- Xiao, M., Ding, J.N., Luo, Y., Zhang, H., Yu, Y., Yao, H., Zhu, Z., Chadwick, D.R., Jones, D., Chen, J., Ge, T., 2022. Microplastics shape microbial communities affecting soil organic matter decomposition in paddy soil. *J. Hazard. Mater.* 431, 128589.
- Xu, B., Liu, F., Cryder, Z., Huang, D., Lu, Z., He, Y., Wang, H., Lu, Z., Brookes, P.C., Tang, C., Gan, J., Xu, J., 2020. Microplastics in the soil environment: Occurrence, risks, interactions and fate - a review. *Crit. Rev. Environ. Sci. Technol.* 50, 2175–2222.
- Yuan, J., Ma, J., Sun, Y., Zhou, T., Zhao, Y., Yu, F., 2020. Microbial degradation and other environmental aspects of microplastics/plastics. *Sci. Total Environ.* 715, 136968.
- Yudina, A., Kuzyakov, Y., 2023. Dual nature of soil structure: the unity of aggregates and pores. *Geoderma* 434, 116478.
- Zhang, X., Li, Y., Ouyang, D., Lei, J., Tan, Q., Xie, L., Li, Z., Liu, T., Xiao, Y., Farooq, T.H., Wu, X., Chen, L., Yan, W., 2021. Systematical review of interactions between microplastics and microorganisms in the soil environment. *J. Hazard. Mater.* 418, 126288.
- Zhang, G.S., Liu, Y.F., 2018. The distribution of microplastics in soil aggregate fractions in southwestern China. *Sci. Total Environ.* 642, 12–20.
- Zhang, L., Xie, Y., Liu, J., Zhong, S., Qian, Y., Gao, P., 2020. An overlooked entry pathway of microplastics into agricultural soils from application of sludge-based fertilizers. *Environ. Sci. Technol.* 54, 4248–4255.
- Zhang, M., Zhao, Y., Qin, X., Jia, W., Chai, L., Huang, M., Huang, Y., 2019. Microplastics from mulching film is a distinct habitat for bacteria in farmland soil. *Sci. Total Environ.* 688, 470–478.
- Zhou, M., Liu, C., Wang, J., Meng, Q., Yuan, Y., Ma, X., Liu, X., Zhu, Y., Ding, G., Zhang, J., Zeng, X., Du, W., 2020. Soil aggregates stability and storage of soil organic carbon respond to cropping systems on black soils of northeast China. *Sci. Rep.* 10, 265.